



PERIOD LENGTHENING CHARACTERISTICS OF TALL BUILDINGS CONSIDERING SOIL STRUCTURE INTERACTION

J. A. Mercado⁽¹⁾, L. G. Arboleda-Monsalve⁽²⁾, K. R. Mackie⁽³⁾

⁽¹⁾ Research Assistant, Dept. of Civil, Environmental, and Construction Engineering, Univ. of Central Florida, Orlando, FL, 32816, USA. E-mail: jamercado@knights.ucf.edu

⁽²⁾ Assistant Professor, Dept. of Civil, Environmental, and Construction Engineering, Univ. of Central Florida, Orlando, FL, 32816, USA. E-mail: luis.arboleda@ucf.edu

⁽³⁾ Professor, Dept. of Civil, Environmental, and Construction Engineering, Univ. of Central Florida, Orlando, FL, 32816, USA. E-mail: Kevin.Mackie@ucf.edu

Abstract

Soil-structure interaction (SSI) has been incorporated in seismic designs of tall buildings to understand the participation of soils in earthquake response of structures. Natural period of the structures can be elongated by the inclusion of a flexible foundation system. Period lengthening arising from the inclusion of SSI changes seismic design of structural and geotechnical systems since period elongation may lead to larger demands in the structure, particularly inter-story drifts. Period lengthening characteristics of structures have been studied by including frequency-dependent springs and dashpots to simulate stiffness and damping characteristics of soils. Numerical models based on direct or continuum approaches can elucidate numerous features of the interaction of nonlinear-inelastic soil-foundation-structure systems, but such robust modeling approaches are still not an integral component of seismic-resistant design of structures, arguably because of their large computational cost and complexity. The objective of this paper is to parametrically study the main variables that influence period lengthening characteristics of tall buildings. These variables include: fixed-base natural period of the buildings, effective structural height, structural aspect ratios, and effective soil shear wave velocity of supporting soils. To accomplish this goal, archetypical models of buildings are developed in OpenSees varying the geometric configuration of the structure in terms of effective height to base ratio, fixed-base first-mode natural period, and dynamic characteristics of the supporting soils. The soil is modeled by means of a direct approach to include a fully-coupled soil-structure system to represent in a more realistic manner the SSI effects. Period lengthening of the first natural period of the structure arising from including SSI effects in the numerical framework produced more flexible structures. The main parameters influencing period lengthening in structures are the geometry of the buildings and the shear wave velocity of the soil.

Keywords: Period Lengthening; Soil-Structure Interaction (SSI); Tall Buildings; Direct Approach.



1. Introduction

Soil-structure interaction should be considered when analyzing the dynamic response of buildings to avoid unrealistic computation of engineering demand parameters that affect seismic designs. The response of buildings to earthquakes is largely affected by the stiffness and damping characteristics of the supporting soils since the building is placed on a flexible foundation system, unrealistically modeled using conventional fixed-base building assumptions. Mylonakis and Gazetas [1] found that the period lengthening of a structure due to SSI did not necessarily produce a conservative response and may lead to larger ductility demands in the structure. SSI generally increases the natural period of the structures by the inclusion of a flexible base soil-foundation system. This is usually referred to as period lengthening. This period lengthening may modify the seismic performance of a building by increasing translation and rotation due to the flexibility of the soil. SSI effects are properly accounted for in seismic response analyses when soil strength and stiffness reduction (i.e., strength-stress-strain soil response), soil damping evolution characteristics, and soil-foundation-structure responses are modeled as a fully coupled system. NIST [2] and Givens [3] summarized several methods to account for SSI effects, including the ‘sub-structure’ and ‘direct’ approaches. They evaluated the period lengthening of a single degree of freedom (SDOF) oscillator with translational and rotational springs at the base, finding general trends of period lengthening and damping in structures due to the soil flexibility. In the direct approach, the structure and soil are represented as a fully coupled system, in which the soil is modeled as a continuum. The computational cost and complexity of the direct approach is large; thus, its use is still limited in practice. However, several authors such as Karimi and Dashti [4], Tomeo et al. [5], Mercado and Arboleda-Monsalve [6], and Arboleda-Monsalve et al. [7] have used direct approaches in their research to evaluate the dynamic characteristics of buildings, finding that SSI affects the distribution of engineering demands in the structure, concluding that oversimplified fixed-base assumptions are not always conservative.

This paper focuses on numerically investigating the effect of structural and soil parameters on period lengthening characteristics of archetypical low-rise to tall buildings. The period lengthening is assessed with eigenvalues analyses in OpenSees [8] using multi-degree of freedom (MDOF) structures supported on soils modeled with linear-elastic formulations. Modification of structural natural periods by means of MDOF considering SSI effects is studied and compared to idealized fixed-base conditions. The main goal is to show how the first-mode natural period is modified with the inclusion of SSI effects. To accomplish this, archetypical models of buildings were developed in OpenSees parametrically varying the geometric configuration of the structure and the characteristic of the supporting soils.

2. Period Lengthening of SDOF Systems

Period lengthening can be easily evaluated with a SDOF oscillator on a flexible base with translational and rotational springs, enabling the system to displace horizontally and rotate at the base [3]. The undamped natural vibration period of a fixed-base oscillator with mass m and stiffness k , can be estimated as $T = 2\pi\sqrt{m/k}$ [9,10]. Considering the same system but supported on vertical, horizontal, and rotational springs at the base with stiffnesses k_z , k_x , and k_{yy} respectively, may be used to represent the flexibility of the supporting soil [2]. Eq. (1) presents the simplified period lengthening ratio (\tilde{T}/T) proposed by Veletsos and Meek [11] that relates the natural period, stiffness, and effective height h of the fixed-base SDOF oscillator with the flexible natural period (\tilde{T}) and the stiffnesses of the supporting springs, as follows:

$$\frac{\tilde{T}}{T} = \sqrt{1 + \frac{k}{k_x} + \frac{kh^2}{k_{yy}}} \quad (1)$$

In Eq. (1), the height of the SDOF should be taken as the height to the center of mass for the first mode shape, which is approximately two-thirds of the total height [12]. It is implicit in the equation that the period lengthening only affects the first mode of vibration and higher vibration modes are not altered. \tilde{T}/T does not seem to be influenced by the structural mass. The horizontal and rotational spring stiffnesses can be calculated



from well-known impedance formulations such those proposed by Pais and Kausel [13], Gazetas [14], and Mylonakis et al. [15], assuming a rigid rectangular foundation at the ground surface.

There are also dimensionless parameters controlling period lengthening in structures, as reported by Veletsos and Nair [16] and Bielak [17]. Those parameters were initially applicable for circular foundations, and NIST [2] adapted them for rectangular foundations. Eq. (2) presents such dimensionless parameters:

$$\frac{h}{TV_s}, \quad \frac{h}{B}, \quad \frac{B}{L}, \quad \frac{m}{4BLh\rho_s}, \quad \text{and} \quad \nu \quad (2)$$

B and L refer to the half-width and half-length of the foundation, m is the mass of the structure, ρ_s is the soil mass density, V_s is the shear wave velocity of the soil, and ν is the Poisson's ratio of the soil. h/TV_s parameter represents the structure-to-soil stiffness ratio. For typical moment frame structures, this parameter is less than 0.1 and for shear wall and braced frame structures it varies between 0.1 and 0.5 [18]. $m/4BLh\rho_s$ parameter is called the mass ratio that relates the mass of the structure to the mass of a certain volume of the soil below the foundation. The mass ratio is commonly taken as 0.15, according to Veletsos and Meek [11]. h/B and B/L are the effective aspect ratios which represent geometric parameters of the soil-structure system.

2. Modeling Assumptions of MDOF Systems

To evaluate the main variables affecting the period lengthening, two-dimensional (2D) MDOF archetypical buildings were developed under fixed and flexible-base support conditions. The building archetypes were varied in width and height to obtain different aspect ratios. Building realizations from one to five bays and from one to 30 stories were simulated in OpenSees. As a result, low-rise and tall buildings were generated. Bay widths and floor heights were assigned constant values, 9.0 and 3.67 m, respectively. This represents h/B values from approximately 0.1 to 18.5. Nodal masses were kept constant among the building realizations (i.e., 44 Mg per node, assuming a slab on metal deck for typical spans and steel frame). In this study, the structural stiffness property was varied to assess how it affects the period lengthening characteristics of tall buildings based on the beam-to-column stiffness ratio (ρ). This ratio controls the mode shape of the buildings and the seismic behavior of the frame, where values close to zero represent a moment-resistant frame and large values represent a shear-resistant frame [19]. ρ was varied from 0.1 to 0.9 times the summation of the inertias (I_b/I_c) at each floor, varying the building type from a flexural to a shear-type lateral response. Young's modulus (E) of the elements was assumed to be constant (i.e., 200 GPa), and thus the inertias were varied to reach the desired ρ . As a result of these variations in the number of bays, number of stories, and ρ , a total of 775 different building configurations were modeled and analyzed using eigenvalue analyses.

Fig. 1 shows the natural periods of the fixed-base structures. Fixed-base natural periods were achieved for each realization based on the ASCE 7-16, Eq. 12.8-7 [12] for moment-resisting frame systems, with $T = 0.0724h_s^{0.8}$, where h_s is the total height of the structure. T was kept constant for structures with the same height and different ρ and number of bays since ASCE 7-16 equation only depends on the height of the structure (e.g., a 10-story building has the same T with two or five bays, and ρ equal to 0.1 or 0.9). Eigenvalue analyses in OpenSees were performed to confirm that the target natural periods were achieved.

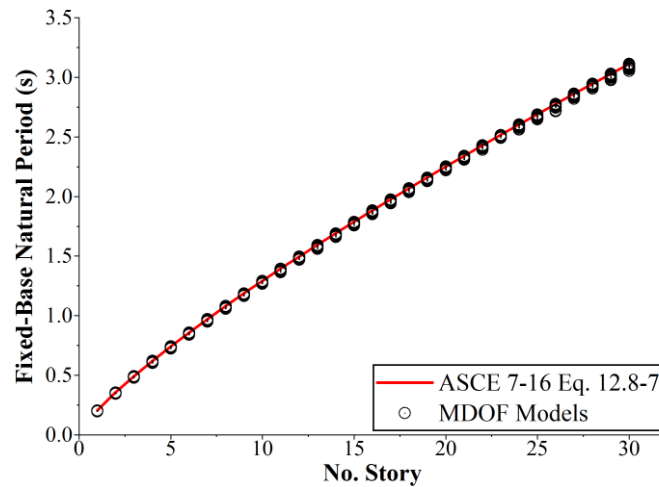


Fig. 1 – Natural periods of the fixed-base building realizations compared to ASCE 7-16 moment-resisting frame equation.

To evaluate the period lengthening, the previous building realizations were placed on a flexible base by means of a direct approach to include a fully coupled soil-structure system. This modeling technique represents a more realistic manner to study SSI effects associated to period lengthening. **Fig. 2** presents a scheme of the variations performed in the soil domain and in the buildings. For the models supported on a flexible soil domain, eigenvalue analyses were performed to compute the \tilde{T} . A mat foundation was added to the base of the buildings as a linear elastic element. Mat foundation nodes were tied to the soil nodes using master/slave node constraints. The boundaries of the soil domain were modeled assuming the nodes are fixed against displacements in the vertical and horizontal directions. These boundaries are only needed to perform eigenvalue analyses to the soil-structure system and they are not representative of a dynamic phase characterized by an earthquake excitation. A 40-m-deep and 250-m-wide size of the soil domain was chosen. The soil domain was modeled using *quad* plane-strain elements. The *ElasticIsotropic* model was used for the soil cluster with elastic properties derived from the assumed shear wave velocities. V_s values varying from 150 to 750 m/s were assigned to the soil domain to reproduce loose to dense soil conditions. The inclusion of the V_s in the building realizations, produced 5,250 MDOF buildings including SSI effects. A Poisson's ratio of 0.33 was used for the analyses.

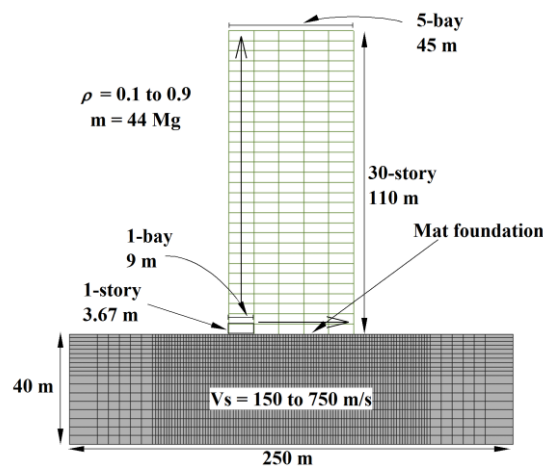


Fig. 2 – Scheme of finite element model with structural and soil variables used in the eigenvalue analyses.



3. Variables Influencing Period Lengthening

The factors potentially influencing period lengthening characteristics of tall buildings were evaluated. **Fig. 3** shows the relation between the period lengthening and the structural parameter ρ . Negligible dependence of the period lengthening on beam-to-column stiffness ratio is shown in the figure. \tilde{T}/T values up to 5.0 were computed with different stiffness characteristics of the structures. This is due to the initial building realization method adopted herein, since the fixed-base natural periods were targeted independently of the ρ and number of bays.

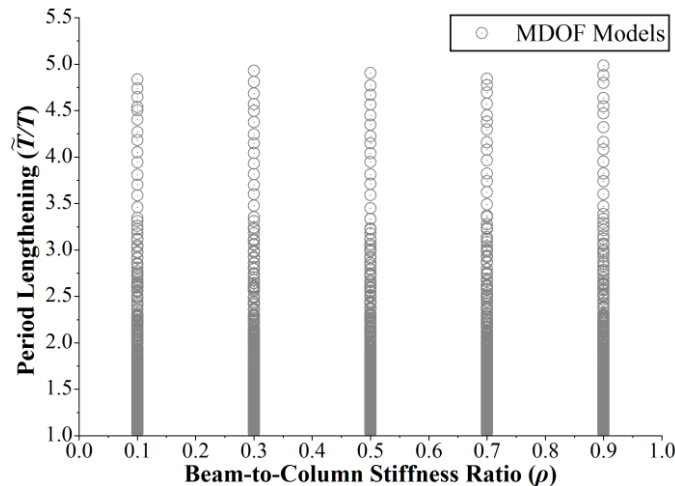


Fig. 3 – Period lengthening variation with ρ defined as the summation of the beam and columns stiffnesses of a story.

Period lengthening in buildings is highly influenced by the structural geometric configuration. **Fig. 4** shows the relationship between period lengthening and effective aspect ratio. As expected, slender buildings with large aspect ratios tend to have large period lengthening ratios. Another parameter that influences \tilde{T}/T is the V_s of the supporting soils. Very flexible soils produced \tilde{T}/T from 1.5 to 5 for low-rise and tall buildings, respectively. Note the large influence of the effective aspect ratio and the shear wave velocity of the soil on the period lengthening.

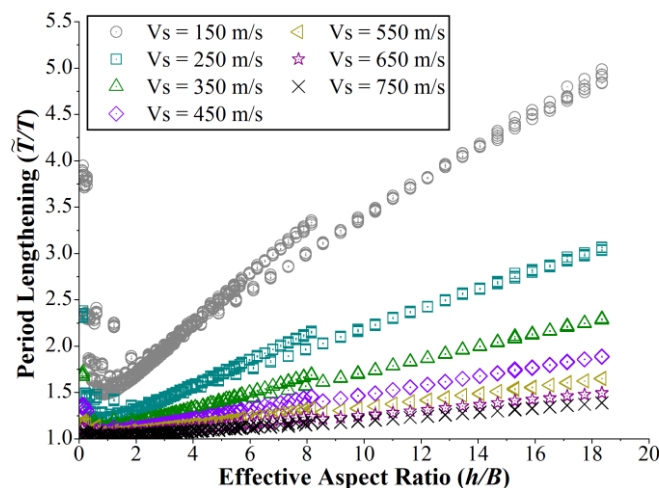


Fig. 4 – Period lengthening variation with the effective aspect ratio and shear wave velocity.

Fig. 5 presents the variation of \tilde{T}/T in terms of geometric characteristics of the structure based on the number of stories and bays. **Fig. 5a** shows that the largest period lengthening values on the structures are for tall buildings. **Fig. 5b** shows a reduction of the \tilde{T}/T values as the number of bays increase (i.e., small effective



aspect ratios). Soil flexibility in buildings tend to increase the rocking motion during an earthquake, however, as the building has more bays, this rocking motion decreases considerably, which is reflected in small \tilde{T}/T values.

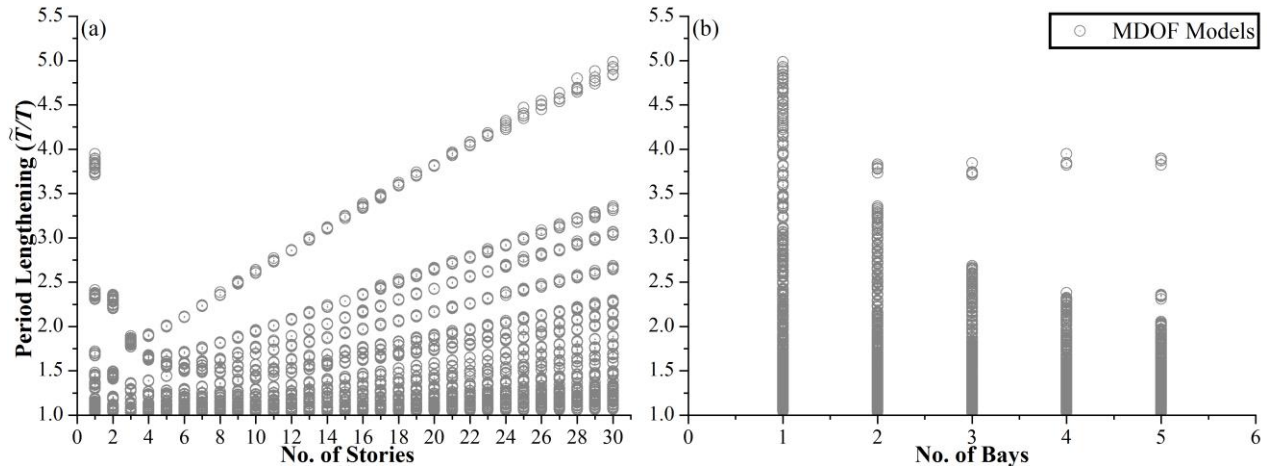


Fig. 5 – Period lengthening variation with the building geometry: a) number of stories and b) number of bays.

Previous dimensionless parameters mostly associated variations in period lengthening with the geometric configuration and stiffness distribution of the structural system. **Fig. 6** presents the variation of period lengthening in terms of predominant shear wave velocity of the supporting soils. Contour lines of h/B are presented in the figure. Note the large influence of the dynamic soil properties and the effective aspect ratio in the \tilde{T}/T of the structures. Soils with large V_s (i.e., “firm” soils) tend to produce small period lengthening due to the decreased soil flexibility and limiting potential of rocking motions. Small \tilde{T}/T values up to 1.5 for a soil with V_s equal to 750 m/s seem plausible even for slender tall buildings (i.e., h/B of 18.5). These tall buildings may have pronounced rocking during an earthquake that a “firm” soil base is able to mitigate. Buildings with small effective aspect ratios on “firm” soils have small or negligible period lengthening values. \tilde{T}/T values up to 5 were computed for slender tall buildings supported on flexible soils with predominant V_s of 150 m/s. It is important to note that the main parameters affecting period lengthening in structures are soil properties and the geometric configuration of the structure.

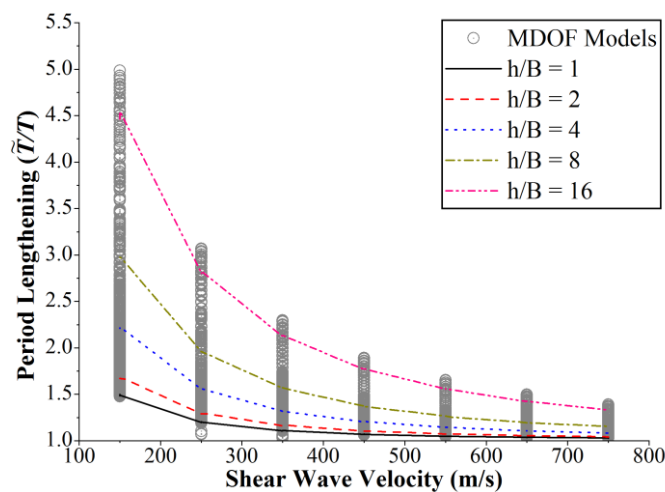


Fig. 6 – Period lengthening variation with the predominant shear wave velocity of the supporting soil.

Fig. 7 shows the variation of \tilde{T}/T with the calculated mass ratio for each building realization. Small and large mass ratios correspond to buildings with five bays and one bay, respectively. Note that the calculated



$m/4BLh\rho_s$ values from the building realizations are in the order of magnitude to the 0.15 reference value cited by Veletsos and Meek [11]. The effect of the mass ratio parameter in the period lengthening seems to be small, although the larger the ratio the larger the period lengthening. The geometry of the building and the V_s are the controlling parameters in the figure, since large \tilde{T}/T values in the figure correspond to slender tall buildings in terms of effective aspect ratios supported on soils with low V_s values of 150 m/s. Note that small mass ratios are associated to small period lengthening for 5-bay buildings. These buildings due to the small effective aspect ratio tend to have small period lengthening.

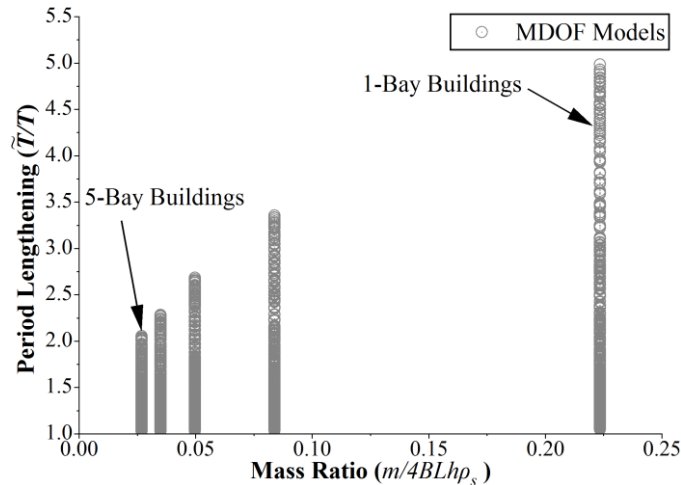


Fig. 7 – Period lengthening variation with mass ratio.

5. Validation of Results

Fig. 8 presents the period lengthening variation with the structure-to-soil stiffness ratio. In the conventional definition of structure-to-soil stiffness ratio, large h/TV_s values are usually associated to shear-type and braced frame structures, which according to the figure, tend to have large period lengthening. \tilde{T}/T value of 5.0 would correspond for example to a single bay 30-story building supported on a soil with a predominant V_s equal to 150 m/s. These conditions are not realistic for tall buildings and thus, the authors decided to find published SSI studies with period lengthening parameters in earthquake records of buildings. Previous studies have stated that period lengthening in tall buildings may be neglected (e.g., NIST [2]). This study demonstrates that tall buildings with specific structural and soil characteristics may be highly influenced by additional flexibility due to the SSI effects. The figure reveals period lengthening characteristics in tall buildings using MDOF systems for structural and supporting soil conditions that largely differ from the SDOF analyses reported by NIST [2].

Several case histories and numerical simulations from previous studies are shown for comparison purposes in Fig. 8. Fu et al. [20], Givens [3], [21], Tavakoli et al. [22], Nghiem and Chang [23], Karapetrou et al. [24], Galal and Naimi [25], Phan et al. [26], and Mercado et al. [27] performed analyses on buildings including SSI effects. These studies presented the fixed-base and flexible-base periods along with the height of the structure and the shear wave velocity of the supporting soil. For example, Galal and Naimi [25], performed nonlinear analyses of hypothetical low-rise and tall buildings with SSI effects varying parametrically the V_s of the soil. From the data presented in that paper, h/TV_s values were calculated for each soil type (i.e., 0.09, 0.05, 0.02, and 0.01 for soil type E, D, C, and B, respectively based on ASCE 7-16). \tilde{T}/T values varying from 2.96 and 1.04 were computed for soil types E and B, respectively. These analyses match the \tilde{T}/T values computed herein.

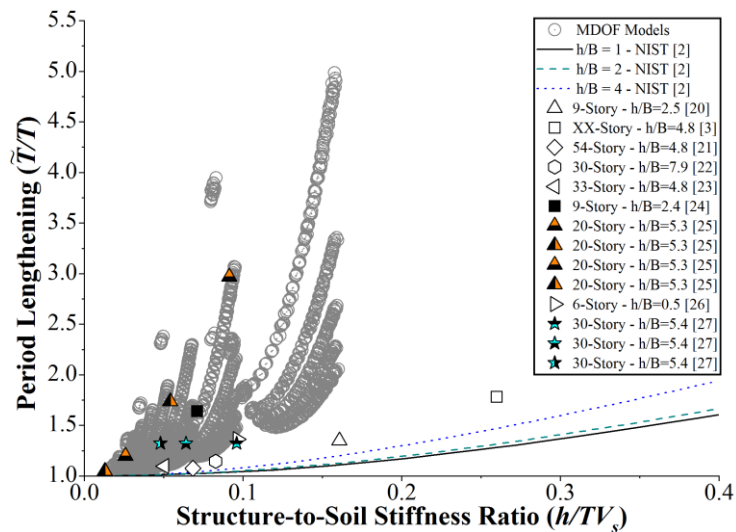


Fig. 8 – Period lengthening variation with the structure-to-soil stiffness ratio.

6. Summary and Conclusions

This paper presented the results of numerical simulations using direct approaches and eigenvalue analyses to assess the period lengthening characteristics of buildings arising from SSI effects. MDOF hypothetical building models including SSI effects were evaluated to determine the main variables influencing the period lengthening of buildings. These parameters included mass ratio, beam-to-column stiffness ratio, effective aspect ratio, number of stories and bays, predominant shear wave velocity of supporting soils, and structure-to-soil stiffness ratio. A parametric variation of the shear wave velocity of the soil and the geometric and stiffness configuration of the structure was performed to assess their contribution to period lengthening. The analyses showed that period lengthening in structures is largely influenced by the predominant shear wave velocity of the supporting soil and the geometric configuration of the structure. Tall buildings with specific geometry and soil profile (i.e., large aspect ratios and loose soils) have large period lengthening values which directly affects the seismic performance.

7. Acknowledgements

Financial support for this work was provided by the National Science Foundation Grant No. CMMI-1563428. The support of Dr. Joy Pauschke and Dr. Richard Fragaszy, program directors at the National Science Foundation, is greatly appreciated.

8. References

- [1] Mylonakis G, Gazetas G. (2000). Seismic Soil-Structure Interaction: Beneficial or Detrimental? *J Earthq Eng* 4:277–301. <https://doi.org/10.1080/13632460009350372>.
- [2] National Institute of Standards and Technology NIST. (2012). Soil-Structure Interaction for Building Structures, Report NIST/GCR 12-917-21. vol. 12. <https://doi.org/12-917-21>.
- [3] Givens MJ. (2013). Dynamic Soil-Structure Interaction of Instrumented Buildings and Test Structures. University of California, Los Angeles.
- [4] Karimi Z, Dashti S. (2016). Seismic Performance of Shallow Founded Structures on Liquefiable Ground: Validation of Numerical Simulations Using Centrifuge Experiments. *J Geotech Geoenvironmental Eng* 142:04016011. [https://doi.org/10.1061/\(ASCE\)GT.1943-5606.0001479](https://doi.org/10.1061/(ASCE)GT.1943-5606.0001479).
- [5] Tomeo R, Pitilakis D, Bilotta A, Nigro E. (2018). SSI effects on seismic demand of reinforced concrete moment



- resisting frames. *Eng Struct* 173:559–72. <https://doi.org/10.1016/j.engstruct.2018.06.104>.
- [6] Mercado JA, Arboleda-Monsalve LG. (2019). Influence of Substructure Levels on the Computed Seismic Performance of Low-Rise Structures. *J Earthq Eng*:1–17. <https://doi.org/10.1080/13632469.2019.1568928>.
- [7] Arboleda-Monsalve LG, Mercado JA, Terzic V, Mackie K. (2020). Soil-Structure Interaction Effects on Seismic Performance and Earthquake-Induced Losses in Tall Buildings. *J Geotech Geoenvironmental Eng*. [https://doi.org/10.1061/\(ASCE\)GT.1943-5606.0002248](https://doi.org/10.1061/(ASCE)GT.1943-5606.0002248).
- [8] McKenna F, Fenves GL, Scott MH, Jeremic B. (2000). Open System for Earthquake Engineering Simulation (OpenSees).
- [9] Clough R, Penzien J. (1995). *Dynamics of Structures*. 3rd Editio. Computers & Structures, Inc.; .
- [10] Chopra AK. (1995). *Dynamics of Structures: Theory and Applications to Earthquake Engineering*. Prentice Hall.
- [11] Veletsos AS, Meek JW. (1974). Dynamic behaviour of building-foundation systems. *Earthq Eng Struct Dyn* 3:121–38. <https://doi.org/10.1002/eqe.4290030203>.
- [12] ASCE. (2017). *Minimum Design Loads and Associated Criteria for Buildings and Other Structures*. Reston, VA: American Society of Civil Engineers; . <https://doi.org/10.1061/9780784414248>.
- [13] Pais A, Kausel E. (1988). Approximate formulas for dynamic stiffnesses of rigid foundations. *Soil Dyn Earthq Eng* 7:213–27. [https://doi.org/10.1016/S0267-7261\(88\)80005-8](https://doi.org/10.1016/S0267-7261(88)80005-8).
- [14] Gazetas G. (1991). Formulas and Charts for Impedances of Surface and Embedded Foundations. *J Geotech Eng* 117:1363–81. [https://doi.org/10.1061/\(ASCE\)0733-9410\(1991\)117:9\(1363\)](https://doi.org/10.1061/(ASCE)0733-9410(1991)117:9(1363)).
- [15] Mylonakis G, Nikolaou S, Gazetas G. (2006). Footings under seismic loading: Analysis and design issues with emphasis on bridge foundations. *Soil Dyn Earthq Eng* 26:824–53. <https://doi.org/10.1016/j.soildyn.2005.12.005>.
- [16] Veletsos AS, Nair V V. (1975). Seismic Interaction of Structures on Hysteretic Foundations. *J Struct Div* 101:109–29.
- [17] Bielak J. (1975). Dynamic behaviour of structures with embedded foundations. *Earthq Eng Struct Dyn* 3:259–74. <https://doi.org/10.1002/eqe.4290030305>.
- [18] Stewart JP, Seed RB, Fenves GL. (1999). Seismic Soil-Structure Interaction in Buildings. II: Empirical Findings. *J Geotech Geoenvironmental Eng* 125:38–48. [https://doi.org/10.1061/\(ASCE\)1090-0241\(1999\)125:1\(38\)](https://doi.org/10.1061/(ASCE)1090-0241(1999)125:1(38)).
- [19] Blume JA. (1968). Dynamic Characteristics of Multistory Buildings. *J Struct Div* 94:377–402.
- [20] Fu J, Todorovska MI, Liang J. (2018). Correction factors for SSI effects predicted by simplified models: 2D versus 3D rectangular embedded foundations. *Earthq Eng Struct Dyn* 47:1963–83. <https://doi.org/10.1002/eqe.3051>.
- [21] Tileylioglu S. (2008). Evaluation of Soil-Structure Interaction Effects from Field Performance Data. University of California, Los Angeles.
- [22] Tavakoli R, Kamgar R, Rahgozar R. (2019). Seismic performance of outrigger–belt truss system considering soil–structure interaction. *Int J Adv Struct Eng* 11:45–54. <https://doi.org/10.1007/s40091-019-0215-7>.
- [23] Nghiem H, Chang N. (2008). Soil-structure interaction effects of high rise buildings. 6th Int Conf Case Hist Geotech Eng:11–6.
- [24] Karapetrou ST, Fotopoulou SD, Pitilakis KD. (2015). Seismic vulnerability assessment of high-rise non-ductile RC buildings considering soil–structure interaction effects. *Soil Dyn Earthq Eng* 73:42–57. <https://doi.org/10.1016/j.soildyn.2015.02.016>.
- [25] Galal K, Naimi M. (2008). Effect of soil conditions on the response of reinforced concrete tall structures to near-fault earthquakes. *Struct Des Tall Spec Build* 17:541–62. <https://doi.org/10.1002/tal.365>.
- [26] Phan LT, Hendrikson EM, Marshall RD, Celebi M. (1994). Analytical Modeling for Soil-Structure Interaction of a 6-Story Commercial Office Building.
- [27] Mercado JA, Mackie KR, Arboleda-Monsalve LG. (2020). Nonlinear Soil-Structure Interaction Analyses of Tall Buildings. *Earthq Eng Struct Dyn*:Under Peer Review.